



Cite this: *Phys. Chem. Chem. Phys.*,
2017, **19**, 2514

Incorporation of aspirin modulates the dynamical and phase behavior of the phospholipid membrane†

V. K. Sharma,^{*a} E. Mamontov,^b M. Ohl^c and M. Tyagi^{de}

Nonsteroidal anti-inflammatory drugs (NSAIDs) are one of the most widely used medications in the world for their analgesic, antipyretic, and anti-inflammatory actions, despite a well-known incidence of a wide spectrum of their adverse effects. To a great extent, beneficial action and side effects of NSAIDs are associated with the interaction of these drugs at the cell membrane level. Here, we use neutron scattering to combine elastic intensity scans, quasielastic and neutron spin echo (NSE) measurements to understand the effect of aspirin, a commonly used NSAID, on the dynamical and phase behavior of the membrane of dimyristoylphosphatidylcholine (DMPC), a prominent representative of phospholipids residing in the outer leaflet of the human erythrocyte membrane. Elastic intensity scans reveal that addition of aspirin not only eliminates the pre-transition (solid gel to ripple phase), but also broadens the main phase transition (ripple to fluid phase) in the membrane. Moreover, the main phase transition becomes shifted toward a lower temperature. These results are found to be consistent with our differential scanning calorimetry measurements. Elastic intensity scans further suggest that aspirin inhibits the membrane from going into the ordered phase and overall induces disorder in the membrane, thus indicating enhancement in the fluidity of the membrane. Quasielastic neutron scattering (QENS) data show that aspirin affects both lateral lipid motion within the leaflet and the localized internal motion of the lipid. Aspirin accelerates both lateral and internal motions, with the more pronounced effect observed for the ordered phase of the neat membrane. Intermediate scattering function as observed by NSE has been analyzed using the Zilman Granek model, which indicates that addition of aspirin alters the bending modulus of the membrane to make the membrane softer. Our study provides a quantitative description of the effect of an archetypal NSAID, aspirin, on the various physical properties of the model biological membrane, which is essential for understanding the complex drug–membrane interaction.

Received 8th September 2016,
Accepted 21st December 2016

DOI: 10.1039/c6cp06202d

www.rsc.org/pccp

Introduction

Nonsteroidal anti-inflammatory drugs (NSAIDs) are among the most widely used medications for their capability in reducing pain, fever, and inflammation.¹ They are also employed in the

main therapy for chronic pathologies such as arthritis or Crohn's disease. NSAIDs work by suppressing the production of prostaglandins through inhibiting the action of enzyme cyclooxygenase (COX). Prostaglandins are chemical messengers which mediate sensation of pain, fever, and inflammation. Prostaglandins formed *via* COX-1 activity promote platelet aggregation whereas formed *via* COX-2 activity mediate pain, inflammation, and fever. However, there is increasing evidence for the actions of NSAIDs beyond the COX pathways and for the interactions with the lipid membranes.^{1,2} NSAIDs are amphiphilic and in general orally ingested, thus, they must interact with the membranes to be absorbed and distributed in the human body. Furthermore, inflammatory processes are instigated at the membrane surface, thus, they might also act on the membrane surface. Hence, the interaction of drugs with cell membrane is inevitable. Although NSAIDs are among the most generally used drugs but the utilization of these drugs is still

^a Solid State Physics Division, Bhabha Atomic Research Centre, Mumbai 400085, India. E-mail: sharmavk@barc.gov.in, vkspthy@gmail.com

^b Chemical and Engineering Materials Division, Neutron Sciences Directorate, Oak Ridge National Laboratory, Oak Ridge, TN 37831, USA

^c Jülich Center for Neutron Science, Oak Ridge, Tennessee 37831, USA

^d National Institute of Standards and Technology Center for Neutron Research, Gaithersburg, Maryland 20899, USA

^e Department of Materials Science and Engineering, University of Maryland, College Park, Maryland 20742, USA

† Electronic supplementary information (ESI) available: Fitted QENS spectra and fitting parameters for all the *Q* values for different concentration of aspirin at 293 K and for DMPC membrane with 6.5 wt% aspirin at 280 and 310 K are supplied. See DOI: 10.1039/c6cp06202d

associated with the occurrence of a wide spectrum of side-effects, such as gastrointestinal toxicity, cardiovascular adverse effects, *etc.*^{1,2} Increasing number of reports suggest that adverse effect of NSAIDs is linked to the interaction of these drugs with membranes in various organ systems.^{1,2} Therefore, studying NSAIDs–membrane interactions has significant importance not only for the understanding of the pharmacological actions of these drugs, but also for the coherent advancement of new approaches to overcome NSAIDs side-effects.¹ Structural, dynamical, and other biophysical properties of cell membranes are susceptible to modification due to interactions with NSAIDs, which has been a subject of interest in medicinal chemistry, biophysics, and pharmacology for the last few decades.^{1–7} Biological membranes consist of a mixture of various lipids, membrane integral proteins, and other small molecules (*e.g.* sterols) which are self-assembled into a heterogeneous structure. Glycerophospholipids are the main structural lipids of eukaryotic membranes, with phosphatidylcholine accounting for more than half of the membrane phospholipids.¹ A saturated phosphatidylcholine, 1,2-dimyristoyl-*sn*-glycero-3-phosphocholine (DMPC) has been used as a model biological membrane to study the interaction with NSAID. It is worthwhile to note that DMPC, just as any other model membrane, may not be an ideal representation of biological membranes. For example, exceptional location of other small molecules (*e.g.* vitamin E and cholesterol) have been observed for DMPC membrane compared to other phosphatidylcholine membrane.^{8,9} Aspirin (acetylsalicylic acid) is one of the most commonly used NSAID as an analgesic and antipyretic to relieve minor pains and reduce fever, respectively.¹⁰ It has been found that aspirin exhibits pronounced selectivity to inhibit COX-1 activity, hence a low dose of aspirin is required for anti-platelet action, which is associated with minimization of blood clot formation and thus reduced blockage of arteries. This application of aspirin has major clinical use to improve the survival of a patient with myocardial infarction. Aspirin is a unique NSAID that is able to inhibit the clotting of blood for a prolonged period (4 to 7 days) compared to only a few hours long inhibition by other NSAIDs. This prolonged effect of aspirin makes it an ideal drug for preventing the blood clots that cause heart attacks and strokes. Using X-ray diffraction, it has been shown⁵ that aspirin affects the human erythrocyte shape. Recently,^{6,7} direct experimental evidence has been presented that aspirin molecules participate in saturated phosphatidylcholine bilayer of DMPC and preferably reside in the head group region of the membrane. Due to incorporation of aspirin, positional disorder in the lipid molecules has been found using X-ray diffraction. The experiments have been carried out on supported multilamellar samples at low level of hydration in the gel phase only.^{6,7} However, not much information is available on the effect of aspirin on the microscopic dynamics of the membrane. Membrane dynamics is known to play a key role in the fluidity and viscoelastic behavior of the membrane and is a prime determinant in a number of processes, such as cell signaling, membrane trafficking, cell division, fusion, permeability, *etc.*^{4,11,12} Hence, it is of key interest to detect subtle changes of the membrane dynamics caused by NSAID's. A membrane exhibits complex dynamical behavior

characterized by a superposition of different motions of individual lipid (*e.g.*, vibrational, conformational, rotation, lateral, flip flop) and whole bilayer (*e.g.*, bending motion and thickness fluctuations). These motions encompass a broad range of time scales, from femtoseconds for molecular vibrations, to a few minutes for the trans-bilayer flip flop, and a wide range of length scales, from a few tens of nanometers for bending motion of the bilayer, to angstroms for local lipid molecule motions.^{13–18} Here, we are interested in the lateral, internal and undulation motions in the membrane, which can be investigated using quasielastic neutron scattering (QENS) and neutron spin echo (NSE) techniques. QENS^{18–30} is one of the most suitable techniques to study microscopic dynamics of the membrane on the time scale of nanosecond to picoseconds and length scale of Angstroms to nanometer. Therefore, it's an ideal tool to study the lateral and internal motion of lipid molecules within the bilayer and has been successfully employed by us for this purpose.^{18,25–28} Effect of various small molecules (ethanol, cholesterol, *etc.*) on the dynamics of DMPC membrane had been studied using QENS technique.^{26,29,30} Lateral diffusion of lipid molecules was found to become slower by a factor of 2 in the gel phase due to incorporation of ethanol.²⁹ However, no significant effect on the dynamics of membrane was observed in the fluid phase due to addition of ethanol. Incorporation of cholesterol was found to restrict the dynamics of membrane in the fluid phase.^{26,30} Neutron spin echo spectroscopy (NSE) is a suitable experimental technique sensitive to bilayer motions in a range of timescales from 100 nanoseconds to 0.1 nanosecond and length scales of 10 Å to 1000 Å.^{31–38} Hence, it is an ideal tool to investigate the bilayer's undulation motions, which characterize the bilayer bending rigidity.^{32–38} NSE had been employed to study the effect of various additives (cholesterol, trehalose) on the bending motion of membrane.^{35–38} Membrane stiffening was observed due to addition of cholesterol. However, no effect on the undulations motion and bending rigidity κ of the membrane was observed due to incorporation of trehalose.³⁶

Here we report the impact of aspirin, a commonly used NSAID, on the dynamical, mechanical, and phase behavior of DMPC membrane as studied using combination of various neutron scattering techniques. Elastic intensity scans show that addition of aspirin significantly alters the phase behavior of the membrane. This observation is supplemented by differential scanning calorimetry (DSC) measurements. The effect of aspirin on the dynamical behavior of the membranes have been investigated over a wide range of time scales (about 5 orders of magnitude), from 0.1 microseconds to picosecond, by combining data from QENS and NSE techniques and discussed here.

Materials and methods

Materials

DMPC lipid powder was purchased from Avanti Polar Lipids (Alabaster, AL). Aspirin and D₂O (99.9%) was procured from Sigma Aldrich (St. Louis, MO) and Cambridge Isotope Laboratories (Andover, MA) respectively.

Preparation of unilamellar vesicles

Unilamellar vesicles of DMPC were prepared using the method as described by us.^{18,26} In brief, appropriate amount of DMPC powder with 0, 6.5 and 13 wt% aspirin (with respect to DMPC lipid) were co-dissolved in chloroform, which was evaporated using the gentle stream of nitrogen gas to obtain lipid films. To remove the residual organic solvent, the lipid films were dried by placing the samples under vacuum (10^{-3} atm) for 14 h at 310 K. Dry lipid films were suspended in the desired amount of D₂O at 310 K and went through 4-freeze-thaw cycles by alternately placing the lipid suspension in a warm water bath (330 K) and in a freezer (253 K). Unilamellar vesicles were prepared by extrusion method in which lipid suspension went through a mini-extruder with a porous polycarbonate membrane (pore diameter \sim 100 nm) more than 31 times. During the extrusion process, the temperature of extruder was kept at \sim 320 K to ensure that DMPC were in the fluid phase. After the extrusion, samples were never cooled below the freezing point of water prior to the measurements. Prepared unilamellar vesicles with and without aspirin were characterized by dynamic light scattering (DLS) technique. DLS experiments carried out using a Wyatt Dawn EOS with a DLS attachment (Wyatt Technology Corp., Santa Barbara, CA) indicated that hydrodynamic radius of the vesicles was uniformly spread around 55 nm. In all the experiments described below the weight ratio of aspirin with respect to DMPC was kept uniform (*i.e.*, 6.5 or 13 wt%), irrespective of the concentration of the DMPC. It should be noted that the desired amount of aspirin was added before hydrating the dry lipid film, not necessarily into the bilayer. A number of studies^{39,40} indicate that aspirin has a high partition coefficient for phosphatidylcholine lipid bilayer. At neutral pH, partition coefficient ($\log_{10}K$) for aspirin in DMPC lipid bilayer is found to be \sim 3.³⁹ Hence, most of the aspirin should be incorporated into the lipid bilayer.

Elastic incoherent neutron scattering

A reactor based backscattering spectrometer such as High Flux Backscattering Spectrometer (HFBS) at the NIST Center for Neutron Research (NCNR), Maryland, with an energy resolution of 0.8 μ eV (FWHM)⁴¹ is an optimal choice for collecting the energy-resolved elastic scattering. Elastic intensity scans have been carried out on 7 (w/w)% DMPC vesicles (with respect to D₂O) with and without 6.5 wt% aspirin (with respect to DMPC) in the same sample holder to ensure that the same amount of DMPC and D₂O is measured in both elastic scans. Standard configuration with Si(111) as monochromator and analyzer crystals corresponding to incident neutron wave length 6.27 Å, has been used. The elastic intensity temperature scan measurements have been carried out with the Doppler monochromator at rest. DMPC membrane undergoes a rather weak pre-transition from the solid gel to ripple phase apart from the strong main phase transition.⁴² Therefore, to investigate both transitions, elastic intensity scan measurements have been carried out from 278 to 306 K in the course of a heating cycle with a slow ramp rate of 0.1 K min⁻¹ to have sufficient statistics

across the transition. At each temperature, count time was set to 2 min, thus providing a very fine temperature resolution increment of 0.2 K.

Quasielastic neutron scattering

QENS measurements have been carried out on 7 (w/w)% DMPC with 0, 6.5 and 13 wt% aspirin using a backscattering spectrometer, BASIS⁴³ at the Spallation Neutron Source (SNS), Oak Ridge National Laboratory (ORNL). BASIS is an indirect geometry neutron spectrometer, with the experimental setup that we used, the spectrometer has an excellent energy resolution of 3.4 μ eV (full width at half-maximum for the *Q*-averaged resolution value) and a range of accessible energy transfers of \pm 100 μ eV suitable for data analysis. The available *Q* range in the chosen set up was 0.3 Å⁻¹ to 1.9 Å⁻¹. This configuration enables access to measure dynamics in the range of time scale from 6 to 400 ps and length scale from 3 to 21 Å. For QENS experiments, the vesicles samples (\sim 2.5 ml) were placed in an annular aluminum sample holders with 0.5 mm internal spacing. These sample holders were selected to give no more than 10% scattering from the samples, thereby minimizing multiple scattering effects. QENS measurements have been carried out at three temperatures namely 310, 293, and 280 K. QENS measurements have also been carried out on pure D₂O at the same temperatures as a reference sample. Besides, to obtain the spectrometer resolution data, QENS measurements were performed on DMPC vesicles at 10 K at the end of the experiment. MANTID software⁴⁴ was used to carry out standard data reduction, which included background subtraction and detector efficiency corrections.

Neutron spin echo

NSE experiments on 1 (w/w)% DMPC with and without 13 wt% aspirin have been carried out at physiological temperature 310 K using NSE spectrometer⁴⁵ at the Spallation Neutron Source (SNS), Oak Ridge National Laboratory. The temperature was controlled by an oil circulation bath with the accuracy of \pm 0.1 K. Vesicles samples (\sim 4 ml) were loaded in Hellma quartz cells having a thickness of 4 mm. A range of wavelength (5–8 Å) was used which enable us to cover the time resolution of Fourier times from 30 ps to 40 ns, and a *Q*-range from 0.05 to 0.13 Å⁻¹. NSE experiments have also been carried out on a standard graphite foil, and D₂O to determine the instrumental resolution and background respectively.

Differential scanning calorimetry

Differential scanning calorimetry (DSC) experiments have been carried out on 3.5 (w/w)% DMPC with and without 6.5 wt% aspirin using a NANO DSC Series III System with Platinum Capillary Cell (TA Instruments). About 300 μ l sample was used for each vesicles and the same amount of D₂O was used for reference. DSC data have been collected for each vesicle in heating as well as in cooling cycle in the temperature range from 280 to 320 K. Scan rate for heating and cooling cycle was 0.5 K min⁻¹. All the DSC measurements have been recorded at 3 atm pressure, to avoid any bubble formation during the scan.

Results and discussion

Elastic intensity scans, or fixed energy-window scans centered at zero energy transfer, is a suitable technique to investigate mobility and phase transitions in a sample *via* temperature scans. Scattered intensity at zero energy transfer within the instrumental resolution (in the present case, 0.8 μeV) can be regarded as purely elastic. Any microscopic mobility in the sample shifts the scattering signal intensity away from zero energy transfer, thereby making the elastic intensity sensitive to the microscopic dynamics. An abrupt loss or gain of intensity in an elastic scan measurement is a signature of a phase transition, which is associated with a change in the microscopic dynamics at the transition temperature. HFBS spectrometer that we utilized to perform elastic intensity scans has 16 detectors, spanning a Q range from 0.25 to 1.75 \AA^{-1} . Monitor normalized Q -averaged elastic intensity (from 0.25 to 1.75 \AA^{-1}) for DMPC membrane with and without 6.5 wt% aspirin measured in a heating cycle is shown in Fig. 1(a). Elastic intensity for DMPC membrane shows two step-like drops at 288 and 297 K, which correspond to the pre- and main phase transition, respectively. It is evident from Fig. 1(a) that elastic intensity for DMPC membrane with aspirin does not show any step-like drop that would correspond to the pre-transition, and the drop in intensity associated with the main transition is not as sharp as the one observed for pure DMPC. This indicates that aspirin significantly affects the phase behavior of the DMPC membranes; the pre-transition is eliminated, and the main transition becomes broad compared to pure DMPC. Moreover, the main phase transition becomes shifted toward lower temperatures and is observed at 292 K. These observations are found to be consistent with the recent small-angle X-ray scattering (SAXS) and wide-angle X-ray scattering (WAXS) on the molecular interaction between different NSAIDs and phosphatidylcholine membrane.³ It was found that NSAIDs abolish the pre-transition indicating a surface-disordering effect of these drugs. Main phase transition was also found to be shifted toward the lower temperature.

DSC measurements have also been carried out on DMPC vesicles with and without 6.5 wt% aspirin, as shown in Fig. 1(b) for a heating and a cooling cycle. It is evident that DSC spectrum for pure DMPC membrane shows a sharp peak around 297 K in the heating cycle, indicating the main phase transition from the ordered phase to the fluid phase. This phase transition is found to be completely reversible on cooling. However, in the presence of 6.5 wt% aspirin, the peak corresponding to the main phase transition becomes significantly broadened and shifted toward the lower temperature. DSC measurements support our elastic intensity scan data, indicating that aspirin has a profound effect on the phase behavior of the membrane.

As mentioned earlier, elastic intensity scan measurements have been carried out on the same concentration of DMPC *ca.* 7 (w/w)% with and without 6.5 wt% aspirin in the same sample holder to ensure the same amount of DMPC and D_2O in the neutron beam. Incoherent scattering signal contribution by 6.5 wt% aspirin is less than 2.5%. It is interesting to note that elastic intensity observed from DMPC with aspirin is always lower compared to that from pure DMPC, indicating that incorporation of aspirin into the membrane perturbs the packing of the lipids into the bilayer resulting in more disorder and concomitantly enhanced dynamics in the membrane. It is evident from Fig. 1(a) that below the main phase transition temperature, elastic intensity from DMPC with aspirin is much lower with respect to the pure membrane. In contrast, above the main phase transition temperature, the difference in the elastic intensities is smaller. This demonstrates that aspirin inhibits DMPC membrane from going into the ordered phase. For quantitative information on the effect of aspirin on the dynamical behavior of the membrane, QENS experiments have been carried out on DMPC vesicles with varying concentration of aspirin at 280, 293 and 310 K, at which temperature points neat DMPC membrane is in the solid gel, ripple, and fluid phase, respectively, as indicated by our elastic scan measurement (Fig. 1(a)). For background subtraction, QENS measurements have also been carried out on D_2O at the same temperatures.

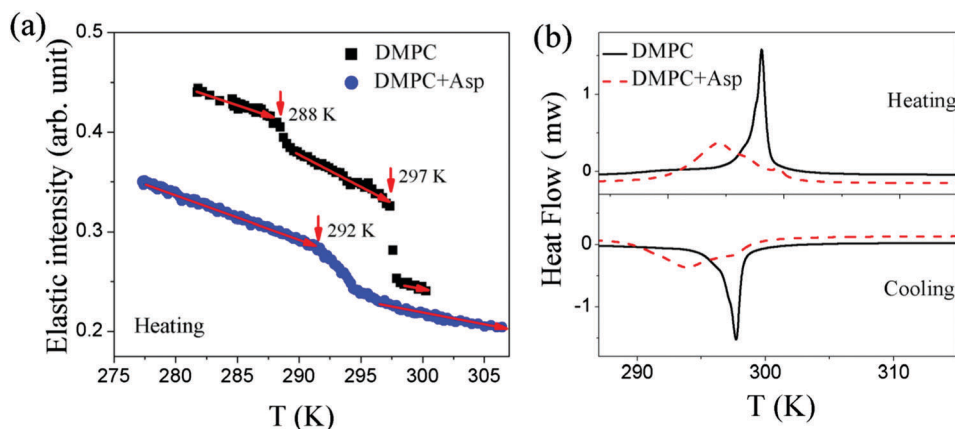


Fig. 1 (a) Monitor normalized Q -averaged (from 0.25 to 1.75 \AA^{-1}) elastic scattering intensity observed from pure DMPC^{27,28} and DMPC with 6.5 wt% aspirin in the heating cycle as measured using HFBS spectrometer ($\Delta E \sim 0.8 \mu\text{eV}$). (b) DSC thermograms of DMPC with and without 6.5 wt% aspirin in heating and cooling cycles.

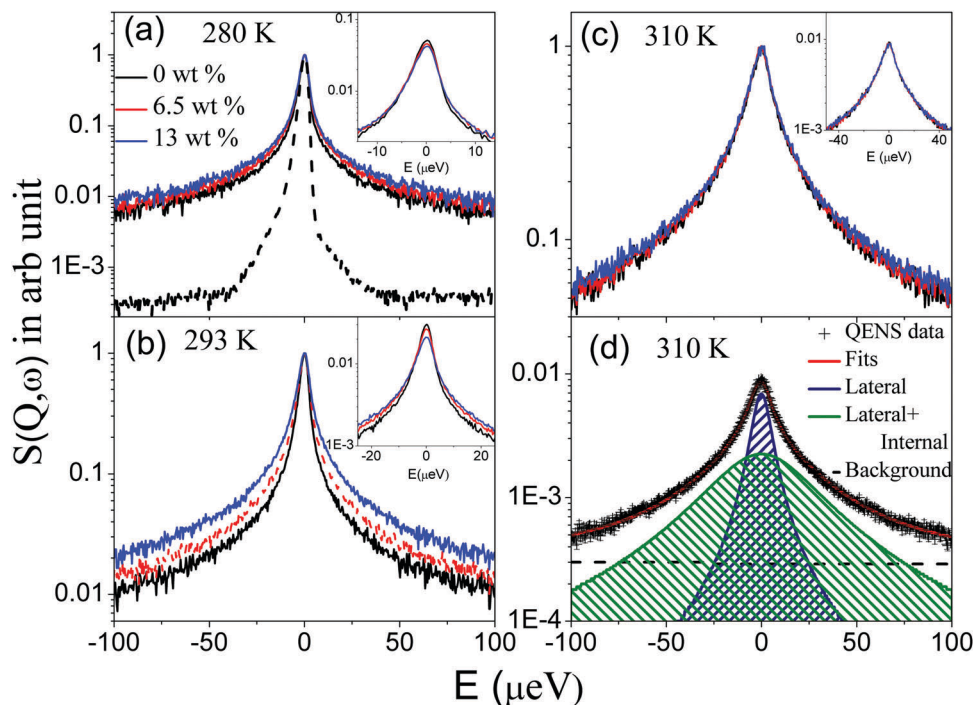


Fig. 2 Peak normalized QENS spectra for DMPC membrane with different concentrations of aspirin at (a) 280, (b) 293 and (c) 310 K at a typical Q value = 1.1 \AA^{-1} . Instrument resolution is shown by dashed line in (a). Significant quasielastic broadening is evident for all samples at the all the measured temperatures. The quasielastic broadening increases with the concentration of the aspirin. For intensity comparison, non-normalized QENS spectra at 280, 293 and 310 K are shown in the inset of (a), (b), and (c), respectively. (d) Typical fitted QENS spectrum for DMPC membrane with 6.5 wt% aspirin at 310 K at $Q = 1.1 \text{ \AA}^{-1}$ using the model scattering law (eqn (4)) convoluted with the instrumental resolution.

Monitor normalized spectra from D_2O are scaled by the volume fraction of the solvent in the vesicles and subtracted from those measured for the vesicle solutions. A representative QENS spectra for DMPC vesicles with different concentrations of aspirin at $Q = 1.1 \text{ \AA}^{-1}$ at 280, 293 and 310 K are shown in Fig. 2(a–c). For a direct comparison of quasielastic broadening with different concentrations of aspirin, the QENS spectra shown in Fig. 2(a–c) are peak normalized by dividing the peak value of each spectra, *i.e.*, $S(Q, \omega)/S(Q, 0)$. For reference, instrument resolution is also shown with the QENS data measured at the lowest temperature *ca.* 280 K. Significant quasielastic broadening is observed for DMPC vesicles with different concentrations of the aspirin at all the measured temperatures. Quasielastic broadening increases with the concentration of aspirin, indicating a progressive acceleration of the dynamics of the membrane by aspirin. The increase in quasielastic broadening is more prominent when the bilayer is in the ordered phase. For intensity comparison, non-normalized QENS spectra have been shown at each temperature in the insets of Fig. 2(a–c). These peak intensities are in agreement with the independently measured elastic intensity scan data as shown in Fig. 1(a).

QENS data for lipid-based systems on nanosecond to picoseconds time scale has been successfully described by two distinct motions (i) the lateral motion of the lipid molecules within the leaflet (\sim ns time scale) and (ii) the internal motion of the lipid molecule (\sim few tens of ps).^{16,26,27} It is generally assumed that these motions are independent from each other.

Therefore, the resultant scattering law for vesicles can be written as^{16,26,27}

$$S_{\text{ves}}(Q, \omega) = S_{\text{lat}}(Q, \omega) \otimes S_{\text{int}}(Q, \omega) \quad (1)$$

where $S_{\text{lat}}(Q, \omega)$ and $S_{\text{int}}(Q, \omega)$ correspond to the scattering functions due to the lateral and internal motions of the lipid molecules, respectively. The lateral motion is characterised by continuous flow diffusion,²⁴ hence the scattering law, $S_{\text{lat}}(Q, \omega)$ can be written as

$$S_{\text{lat}}(Q, \omega) = L_{\text{lat}}(\Gamma_{\text{lat}}, \omega) = \frac{1}{\pi} \frac{\Gamma_{\text{lat}}}{\Gamma_{\text{lat}}^2 + \omega^2} \quad (2)$$

Here Γ_{lat} is the half width at half maximum (HWHM) of the Lorentzian corresponding to the lateral motion of the lipid molecules.

The internal motions are locally confined as restricted by the molecular structure of the lipid molecule, hence there exists a finite probability of finding the scatterer within the chain volume even after a relatively long relaxation time. This gives rise to an elastic contribution to the scattering law. Therefore, the scattering law for the internal motion, $S_{\text{int}}(Q, \omega)$ can be written as

$$S_{\text{int}}(Q, \omega) = A(Q)\delta(\omega) + (1 - A(Q))L_{\text{int}}(\Gamma_{\text{int}}, \omega) \quad (3)$$

where the first term in eqn (3), $A(Q)\delta(\omega)$, represents the elastic part and the second term represents the quasielastic component, which was approximated by a single Lorentzian function, $L_{\text{int}}(\Gamma_{\text{int}}, \omega)$ with half width at half maximum (HWHM), Γ_{int} .

The fraction of the elastic scattering, with respect to the total scattering is known as Elastic Incoherent Structure Factor (EISF). Hence, $A(Q)$ in eqn (3) is nothing but the EISF, which provides information about the geometry of the internal motion.

Hence, the resultant scattering law for vesicles can be written as

$$S_{\text{ves}}(Q, \omega) = L_{\text{lat}}(\Gamma_{\text{lat}}, \omega) \otimes [A(Q)\delta(\omega) + (1 - A(Q))L_{\text{int}}(\Gamma_{\text{int}}, \omega)] \\ = [A(Q)L_{\text{lat}}(\Gamma_{\text{lat}}, \omega) + (1 - A(Q))L_{\text{tot}}(\Gamma_{\text{lat}} + \Gamma_{\text{int}}, \omega)] \quad (4)$$

For data fitting, eqn (4) was convoluted with the instrumental resolution function as measured with a vanadium standard, and the parameters $A(Q)$, Γ_{lat} and Γ_{tot} were determined by a least squares fit of the measured spectra. No parameter is constrained or fixed during the fitting. As Γ_{lat} is already known, Γ_{int} is obtained by subtracting Γ_{lat} from the Γ_{tot} . The data were fitted using the program DAVE⁴⁶ developed at the NIST Center for Neutron Research. It has been found that the model scattering law described well all of the observed QENS spectra for DMPC vesicles with different concentrations of aspirin at all the measured temperatures and Q values.⁴⁷ A typical fitted QENS spectrum for DMPC vesicles with 6.5 wt% aspirin at 310 K is shown in the Fig. 2(d). For detailed quantitative information regarding the lateral and internal motions, the

parameters obtained from the fit *ca.* $A(Q)$, Γ_{lat} , and Γ_{int} are analysed as a function of Q .

Lateral motion

The lateral motion of lipid within the leaflet is of paramount interest since it plays a principal role in various physiologically relevant membrane processes, such as cell signaling, membrane trafficking, cell recognition, location and activity of membrane proteins, protein-protein interaction, *etc.* HWHM of Lorentzian representing the lateral motion, Γ_{lat} is shown in Fig. 3(a). It is evident that Γ_{lat} increases linearly with Q^2 , passing through the origin, thus indicating lateral motion of lipid molecules undergo continuous diffusion. Fick's law is used to determine the lateral diffusion coefficient for all the vesicles at all the measured temperatures and shown in Fig. 3(b). It is evident that aspirin accelerates the lateral motion of the lipid molecules in dose-dependent manner. As the concentration of aspirin is increased, the lateral diffusion coefficient of the lipids increases. Interestingly, the effect of aspirin on the lateral motion strongly depends on the phase of the neat membrane as it is found to be more pronounced in the ordered phase. For example, at 293 K, for pure DMPC membrane, D_{lat} is found to be $1.5 \times 10^{-7} \text{ cm}^2 \text{ s}^{-1}$ which increases with the aspirin concentrations, and at 13 wt% aspirin, it is found to be $2.5 \times 10^{-7} \text{ cm}^2 \text{ s}^{-1}$ (about 67% higher than for pure membrane). However, at 310 K, where lipids are

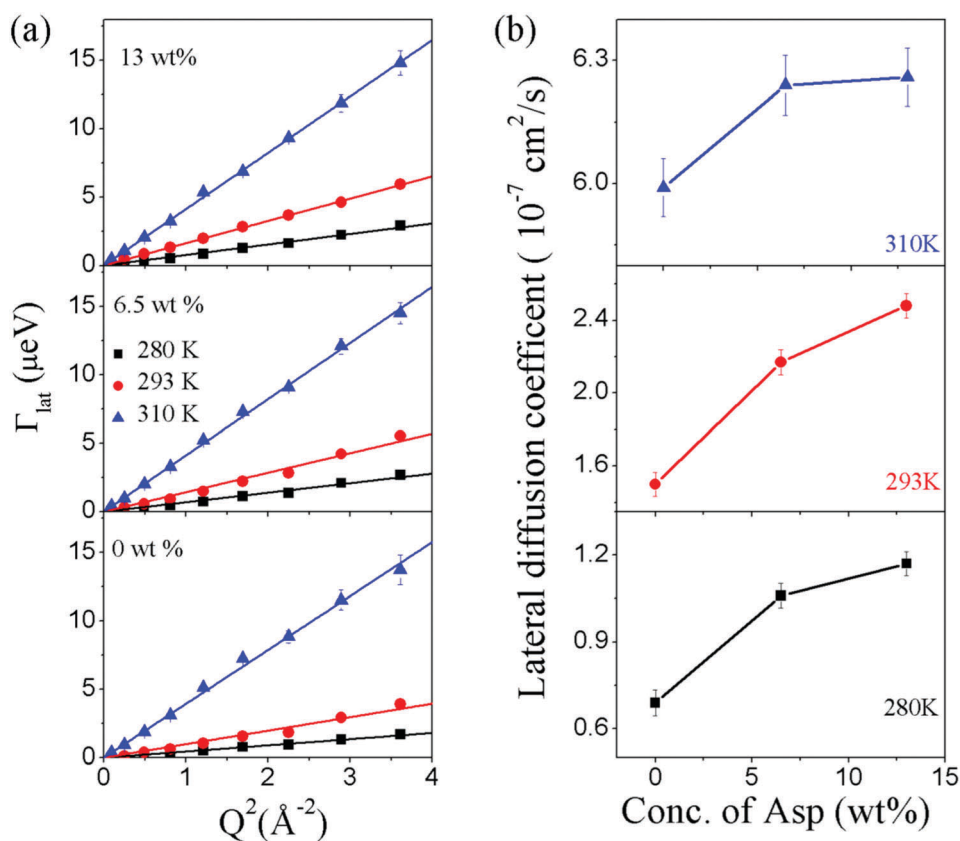


Fig. 3 (a) Variation of HWHM of the Lorentzian corresponding to lateral motion with Q^2 for DMPC membrane with different concentrations of aspirin. Solid lines are the fits correspond to Fick's law of diffusion. (b) Effect of aspirin concentration on the lateral diffusion coefficient as extracted from the slope of data in (a). Error bars throughout the text represent one standard deviation.

in the fluid phase, the lateral diffusion coefficient is found to increase modestly for 6.5 wt% aspirin and then saturate at 13 wt% aspirin. For pure membrane, D_{lat} is found to be $6.0 \times 10^{-7} \text{ cm}^2 \text{ s}^{-1}$, which increases to $6.3 \times 10^{-7} \text{ cm}^2 \text{ s}^{-1}$ (about 5% higher) for the membrane supplemented with 6.5 wt% aspirin. It is evident from Fig. 3(a) that for pure membrane there is a jump in the HWHM of lateral motion when one goes from 293 K to 310 K. However, as the content of aspirin is increased, this jump in HWHM reduces. This observation is consistent with the independent elastic intensity scan measurement, which indicates that due to addition aspirin, main phase transition gets broadened. Elastic intensity carried out at HFBS ($\sim 0.8 \text{ } \mu\text{eV}$) should be most sensitive to the slower lateral motion ($\sim \text{ns}$).

Internal motion

A faster internal motion of lipid along with the lateral motion has been observed with the QENS data measured at BASIS. Internal motion of lipid molecules exhibits complex dynamical behavior, with a superposition of different motions including rotation of lipid molecules, head group motion, segmental motion, out of plane fluctuation, conformational motion, *etc.* It is difficult to separate all of these motions and model them individually from one data set with finite energy resolution and limited energy-transfer range. Hence, the description of the internal motion provided here is given in the context of investigating the effect of

aspirin on the internal dynamics of membrane. Elastic incoherent structure factor (EISF) of the internal motion, represented by the parameter $A(Q)$, and HWHM, Γ_{int} , corresponding to the internal motion for DMPC membrane with different concentrations of aspirin are shown in Fig. 4 at 280, 293 and 310 K. It is evident from Fig. 4 that incorporation of aspirin does have significant effect on the internal motions, especially evident in the ordered phase. It is clear from Fig. 4(a) that in the ordered phase (at 280 and 293 K), as the concentration of aspirin is increased, the corresponding EISF decreases, indicating that incorporation of aspirin enhances the flexibility of the lipid molecules. No significant effect on the EISF due to addition of aspirin is observed when the membrane is in the fluid phase. While comparing QENS signal broadening (Fig. 4(b)), it is found that as the concentration of aspirin is increased, the HWHM, Γ_{int} , increases, suggesting faster internal motions of the lipid molecules. The increase in the HWHM due to addition of aspirin is more prominent when the membrane is in the ordered phase. Hence, our measurements suggest that incorporation of aspirin makes lipid molecules more flexible and enhances the internal dynamics. Enhancement in flexibility and dynamics due to addition of aspirin is more prominent when membrane is in the ordered phase.

Thus, aspirin is found to enhance both lateral and internal motions of the DMPC molecules. Recently, Rheinstadter group

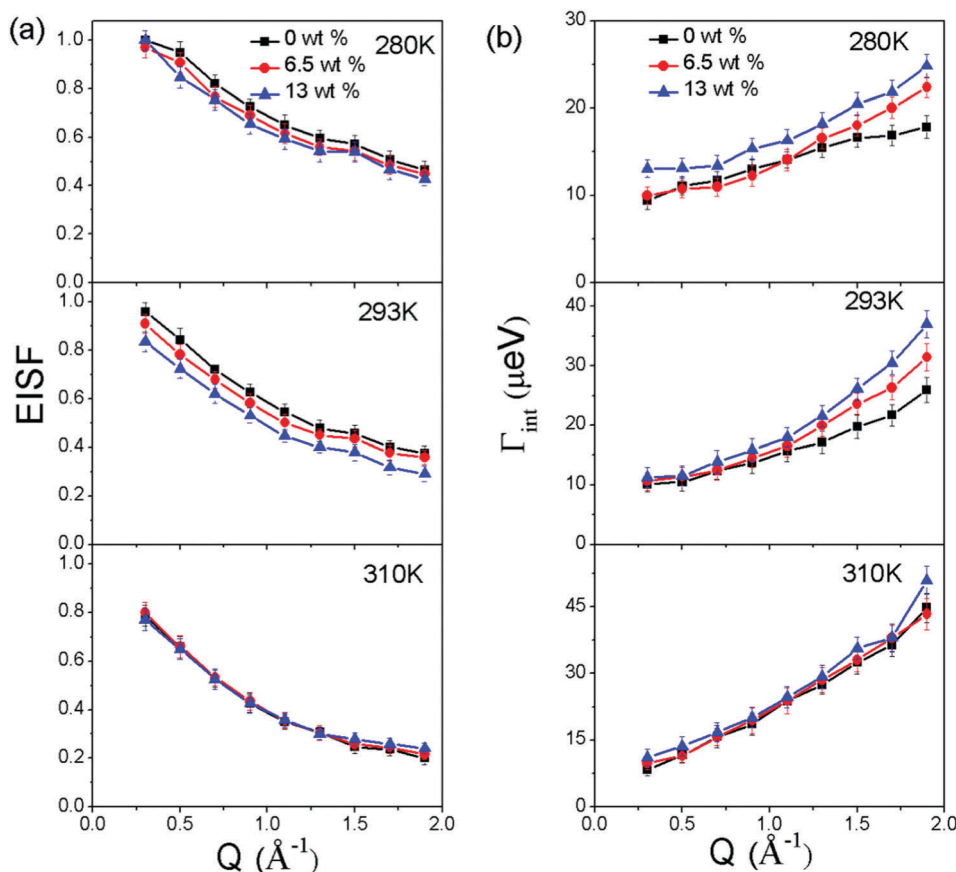


Fig. 4 Variation of (a) EISF and (b) HWHM of the Lorentzian corresponding to internal motion with Q for DMPC membrane with different concentrations of aspirin at 280, 293 and 310 K.

has shown^{6,7} that for DMPC membrane, aspirin is located near the head group in an orientation such that oxygen groups are pointing towards the hydration water. This orientation protects the hydrophobic part of the aspirin molecule from the aqueous environment. It is also found that aspirin located near the head groups creates an increased disorder of the acyl chains, *i.e.*, a higher number of *gauche* defects in the hydrocarbon chains. These reports are consistent with our present results that inclusion of aspirin enhances the internal motion of DMPC.

Undulation motion

Undulation motion is characterized by the bending rigidity of the membrane. Bending modulus has a prominent role in a number of membrane processes such as cell division, fusion, shape changes, adhesion, and permeability. To investigate the impact of aspirin on the bending motion, NSE experiments have been carried out on DMPC membrane with and without aspirin. The normalized intermediate scattering function for DMPC membrane with and without aspirin as observed by NSE is shown in Fig. 5. Zilman Granek (ZG) model⁴⁸ has been employed to explain the observed intermediate scattering functions. This model is valid in the Q range of $QR_{\text{ves}} \gg 1$, where R_{ves} is the radius of vesicles. For the present NSE experiment, the radius of unilamellar vesicles (R_{ves}) is ~ 500 Å; hence, the condition $QR_{\text{ves}} \gg 1$ is satisfied for the used Q range. According to ZG model, the time decay of intermediate scattering function, $I(Q,t)$ of a free-standing membrane due to thermal

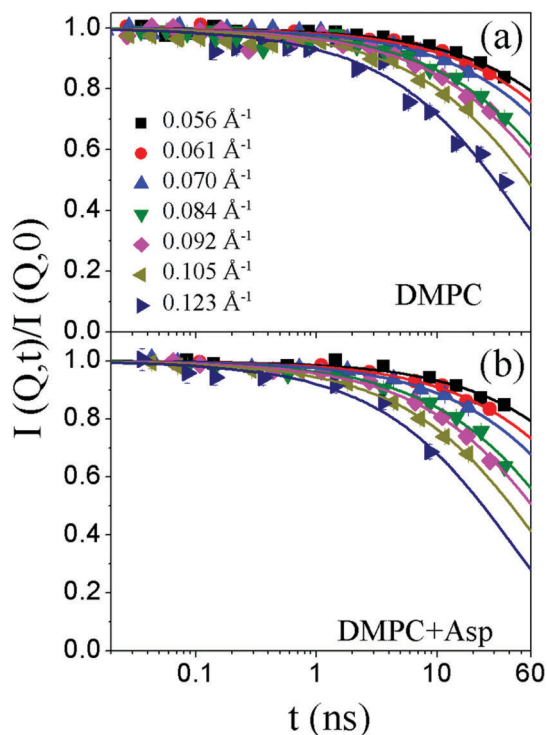


Fig. 5 Observed intermediate scattering functions for (a) neat DMPC membrane and (b) DMPC membrane with 13 wt% aspirin at 310 K. Solid lines are the fits using the eqn (5).

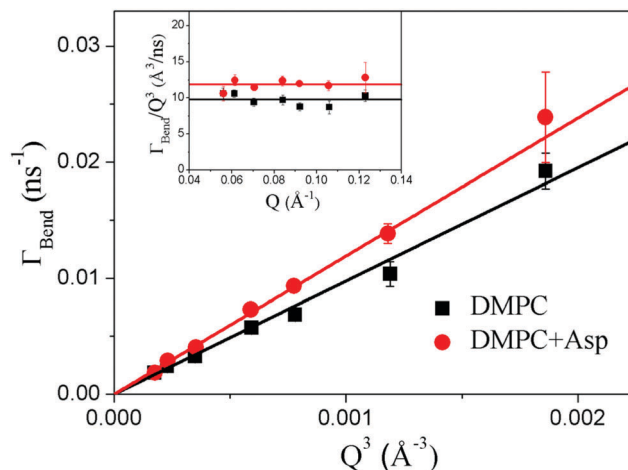


Fig. 6 Variation of relaxation rate corresponding to collective undulation motion, Γ_{Bend} , with Q^3 . Solid lines correspond to linear fits according to ZG model. Inset shows variation of Γ_{Bend}/Q^3 with Q for DMPC membrane with and without 13 wt% aspirin.

undulations can be described as a stretched exponential decay and given as

$$I(Q,t) = I(Q,0)\exp[-(\Gamma_{\text{Bend}}t)^{2/3}] \quad (5)$$

Here Γ_{Bend} is the relaxation rate for the bending motion given as

$$\Gamma_{\text{Bend}} = 0.025\gamma_k \left(\frac{K_B T}{\kappa}\right)^{1/2} \frac{K_B T}{\eta} Q^3 \quad (6)$$

Here, κ is bending modulus of the lipid bilayer, η is the solvent viscosity, K_B is Boltzmann's constant, T is the temperature, and γ_k is a pre-factor. Pre-factor γ_k is a function of $\kappa/K_B T$ and approaches unity for $\kappa/K_B T \gg 1$, which is valid for the lipid bilayer.^{32–34,49} It is evident from Fig. 5 that eqn (5) describes the data well for DMPC membrane with and without aspirin, and the so obtained Γ_{Bend} is shown in Fig. 6. Γ_{Bend} follows a Q^3 dependence (Fig. 6), as expected from the ZG model. It is evident from Fig. 6 that Γ_{Bend} values for membrane supplemented with aspirin is consistently larger *vis-à-vis* pure DMPC membrane, indicating that incorporation of aspirin enhances the bending motion, resulting in the softer membrane. In principle, the bending modulus of the membrane with and without aspirin can be extracted from the slope between Γ_{Bend} and Q^3 using eqn (6). However, a previous study³² has indicated that bending modulus κ obtained using this approach is almost 9 times higher than the expected value for lipid membrane. To account for this discrepancy, an effective solvent viscosity, η_{eff} , which is 3 times the bulk solvent viscosity, is generally used to estimate the value of bending modulus.^{33,34} This discrepancy has been explained recently by Watson and Brown⁵⁰ by considering the effect of local dissipation within the membrane on the length and time scale observable with NSE. In this extended ZG theory, bending modulus κ is replaced by effective bending modulus $\tilde{\kappa} = \kappa + d^2 k_b$,³² where d is the height of the neutral surface from the bilayer mid plane and k_b is the bilayer compressibility modulus. While the exact

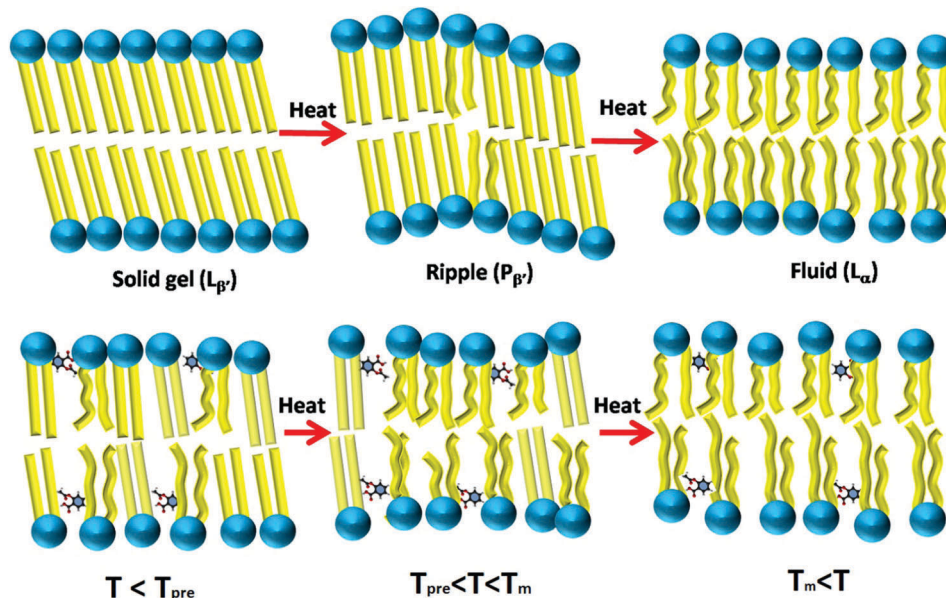


Fig. 7 Schematic of lipid bilayer in neat DMPC membrane (top) and DMPC membrane with aspirin (bottom) in different temperature regimes.

value of d cannot be observed experimentally, it should be close to the half bilayer thickness. Bilayer compressibility modulus k_b and bending modulus of lipid bilayer κ are known to be related to each other, and for saturated lipid bilayer such as DMPC, $k_b = 24\kappa/d_t^2$,^{32,49,51} where d_t is the thickness of the chain region. For the similar lipid system³² $2d/d_t = 1.21$ is used, and, therefore, employed the same relationship for our system. At 310 K, the viscosity of D₂O is 0.84 cP.⁵² Using the value of viscosity, d/d_t , and γ_k , bending modulus for lipid bilayer can be obtained using eqn (6). For DMPC membrane at 310 K, bending modulus is found to be $(17.4 \pm 0.9)K_B T$, which is consistent with the value observed for similar membrane system in the fluid phase.³² The addition of aspirin makes membrane softer, as its bending modulus is found to reduce to $(11.7 \pm 0.4)K_B T$. Our measurement indicates that addition of 13.5 wt% aspirin makes membrane softer, reducing its bending modulus by about 33%.

In summary, we have investigated the effect of aspirin on the phase behavior and microscopic dynamics of a phospholipid membrane over a wide range of time scale covering 5 orders of magnitude, from 100 ns to ps. Our elastic neutron scattering intensity scans and DSC results indicate that aspirin significantly affects the phase behavior of the membrane. A schematic of the lipid bilayer in all three phases, solid gel, ripple, and fluid is shown in Fig. 7. In the gel phase ($L_{\beta'}$), all acyl chains are well ordered, tilted and in *trans* form. As the temperature is increased, there is a weak, pre-transition from the solid gel to the ripple phase, in which lipids act less cooperatively, and a periodic ripple has formed. Upon further increase in temperature, a strong main phase transition is observed, in which acyl chains are disordered and have *gauche* defects. Various properties of the membrane, such as free area per lipid, bilayer thickness, lateral diffusion, *etc.*, undergo an abrupt change across the main phase transition.^{18,53} The addition of aspirin in the membrane creates disorder in the membrane even in the

gel phase, resulting in a large free area and more *gauche* defects in the acyl chain *vis-à-vis* neat membrane. No pre-transition from the solid gel to the ripple phase exists anymore in the elastic intensity scan of DMPC membrane with aspirin. This might be due to either inhibition of the formation of periodic ripple phase, or general waning of the pre-transition because of introduced disorder. The main phase transition becomes significantly broadened and shifted toward the lower temperature due to the incorporation of aspirin. This can be explained on the grounds of the membrane disordering effect as observed by small angle scattering studies^{3,4} and the presence of aspirin preventing lipids cooperative actions. Our QENS and NSE results show that aspirin has a profound effect on the microscopic dynamics of the membrane, accelerating lateral, internal, and undulation motions, which results in a softer and more fluidic membrane. Disordering or fluidizing effect on the membrane increases with the concentration of aspirin and strongly depends on the phase of the membrane. Maximum disordering in the membrane was observed at temperatures when the neat membrane is in the ordered phase. These observations are in agreement with the recent SAXS and WAXS measurements that indicate that NSAIDs produce distinct biophysical effects depending on the initial organization of the membrane.³ Because of the addition of aspirin, bending rigidity of the membrane decreases. This could be understood and explained by the combination of reduced hydration of the head groups and a decrease in bilayer thickness due to the addition of drugs, as indicated by small angle neutron scattering (SANS) study.⁴ The results reported here for aspirin are in stark contrast with the results previously observed for cholesterol, which restricts the dynamics of membrane.^{26,30,35} This can be explained as cholesterol having a condensation effect on the lipid membrane, which suppresses lipid molecular motions, thereby increasing membrane thickness and reducing membrane fluidity.

Conclusions

Incorporation of aspirin is found to enhance all measured components of the microscopic lipid dynamics in DMPC membrane, from fastest localized lipid motion, to slower lateral lipid motion, to the lipid membrane undulations on the time scale of up to 100 ns. Interestingly, aspirin appears to have a plasticizing effect on the DMPC membrane dynamics not only on all the measured time scales, but also in both the gel and fluid phase states of the membrane. Compared to the previous studies^{26–30} of the effect of additives such as cholesterol, melittin, α -tocopherol, or ethanol on DMPC microscopic dynamics, this latter observation is rather unusual. It is rather common for additives to plasticize the gel phase through suppression of lipid ordering, but in the fluid phase the opposite stiffening effect (or at least lack of any effect on the microscopic dynamics) tends to be observed. Aspirin, however, retains plasticizing (albeit weaker) effect on DMPC even in the fluid phase. Even though the effects of NSAIDs on the dynamics of membrane depend on various factors, including concentration and charge of drugs, initial organization of the membrane, pH, interaction between drugs and membrane, *etc.*, we suggest that the universal plasticizing effect of aspirin may be associated with its location near the head groups and its interaction with the membrane, which differentiate aspirin from the previously studied additives. Aspirin is known to create an increased disorder of the acyl chains, *i.e.*, a higher number of *gauche* defects in the hydrocarbon chains. Besides, residence near the head groups may suppress lipid ordering while at the same time avoiding interaction with the lipid tails, thus resulting in a universal plasticizing effect. Although from physiological stand point the main action of aspirin is through the irreversible inhibition of cyclooxygenase that catalyzes the formation of prostaglandins and thromboxanes, the potential effect of aspirin on the flexibility and fluidity (thus, permittivity) of membranes should not be discounted when considering beneficial and side effects of this common medicine.

Acknowledgements

Experiments on HFBS at NCNR are supported in part by the National Science Foundation under Agreement No. DMR-1508249. Research conducted at ORNL's Spallation Neutron Source was sponsored by the Scientific User Facilities Division, Office of Basic Energy Sciences, U.S. Department of Energy. Certain commercial material suppliers are identified in this paper to foster understanding. Such identification does not imply recommendation or endorsement by the National Institute of Standards and Technology, nor does it imply that the materials or equipment identified are necessarily the best available for the purpose.

References

- 1 C. P. Leite, C. Nunes and S. Reis, *Prog. Lipid Res.*, 2013, **52**, 571–584.
- 2 H. E. Vonkeman and M. A. F. J. Van de Laar, *Semin. Arthritis Rheum.*, 2010, **39**, 294–312.

- 3 C. Nunes, G. Brezesinski, J. L. F. C. Lima, S. Reisa and M. Lucio, *Soft Matter*, 2011, **7**, 3002.
- 4 M. B. Boggara and R. Krishnamoorti, *Langmuir*, 2010, **26**, 5734–5745.
- 5 M. Suwalsky, J. Belmar, F. Villena, M. J. Gallardo, M. Jemiola-Rzeminska and K. Strzalka, *Arch. Biochem. Biophys.*, 2013, **539**, 9–19.
- 6 M. A. Barrett, S. Zheng, G. Roshankar, R. J. Alsop, R. K. R. Belanger, C. Huynh, N. Kučerka and M. C. Rheinstädter, *PLoS One*, 2012, **7**, e34357.
- 7 R. J. Alsop, M. A. Barrett, S. Zheng, H. Diesa and M. C. Rheinstädter, *Soft Matter*, 2014, **10**, 4275.
- 8 G. Pabst, N. Kučerka, M. P. Nieh, M. C. Rheinstädter and J. Katsaras, *Chem. Phys. Lipids*, 2010, **163**, 460–479.
- 9 D. Marquardt, J. A. Williams, J. J. Kinnun, N. Kučerka, J. Atkinson, S. R. Wassall, J. Katsaras and T. A. Harroun, *J. Am. Chem. Soc.*, 2014, **136**, 203–210.
- 10 P. A. Mackowiak and A. Philip, *Clin. Infect. Dis.*, 2000, **31**, 154–156.
- 11 D. B. Goldstein, *Annu. Rev. Pharmacol. Toxicol.*, 1984, **24**, 43–64.
- 12 E. J. M. Helmreich, *Biophys. Chem.*, 2002, **100**, 519–534.
- 13 R. Lipowsky and E. Sackmann, *Structure and Dynamics of Membranes From Cells to Vesicles. Handbook of Biological Physics*, Elsevier, North Holland, Amsterdam, 1995, vol. 1.
- 14 J. F. Tocanne, L. D. Ciézanne and A. Lopez, *Prog. Lipid Res.*, 1994, **33**, 203–237.
- 15 R. Macháň and M. Hof, *Biochim. Biophys. Acta*, 2010, **1798**, 1377–1391.
- 16 S. Busch, C. Smuda, L. C. Pardo and T. Unruh, *J. Am. Chem. Soc.*, 2010, **132**, 3232–3233.
- 17 A. C. Woodka, P. D. Butler, L. Porcar, B. Farago and M. Nagao, *Phys. Rev. Lett.*, 2012, **109**, 058102.
- 18 V. K. Sharma, E. Mamontov, D. B. Anunciado, H. O'Neill and V. Urban, *J. Phys. Chem. B*, 2015, **119**, 4460–4470.
- 19 M. Bée, *Quasielastic Neutron Scattering*, Adam Hilger, Bristol, 1988.
- 20 V. K. Sharma, S. Mitra, M. Johnson and R. Mukhopadhyay, *J. Phys. Chem. B*, 2013, **117**, 6250–6255.
- 21 V. K. Sharma, S. Mitra, V. Garcia Sakai, P. A. Hassan, J. Peter Embs and R. Mukhopadhyay, *Soft Matter*, 2012, **8**, 7151–7160.
- 22 V. K. Sharma, S. Mitra, G. Verma, P. A. Hassan, V. Garcia Sakai and R. Mukhopadhyay, *J. Phys. Chem. B*, 2010, **114**, 17049–17056.
- 23 C. L. Armstrong, M. D. Kaye, M. Zamponi, E. Mamontov, M. Tyagi, T. Jenkins and M. C. Rheinstädter, *Soft Matter*, 2010, **6**, 5864–5867.
- 24 C. L. Armstrong, M. Trapp, J. Peters, T. Seydel and M. C. Rheinstädter, *Soft Matter*, 2011, **7**, 8358–8362.
- 25 D. K. Rai, V. K. Sharma, D. Anunciado, H. O'Neill, E. Mamontov, V. Urban, W. T. Heller and S. Qian, *Sci. Rep.*, 2016, **6**, 30983.
- 26 V. K. Sharma, E. Mamontov, D. B. Anunciado, H. O'Neill and V. S. Urban, *Soft Matter*, 2015, **11**, 6755–6767.
- 27 V. K. Sharma, E. Mamontov, M. Tyagi and V. S. Urban, *J. Phys. Chem. B*, 2016, **120**, 154–163.

- 28 V. K. Sharma, E. Mamontov, M. Tyagi, S. Qian, D. K. Rai and V. S. Urban, *J. Phys. Chem. Lett.*, 2016, **7**, 2394–2401.
- 29 L. Toppozini, C. L. Armstrong, M. A. Barrett, S. Zheng, L. Luo, H. Nanda, V. G. Sakai and M. C. Rheinstädter, *Soft Matter*, 2012, **8**, 11839.
- 30 S. Busch and T. Unruh, *Biochim. Biophys. Acta*, 2011, **1808**, 199–208.
- 31 F. Mezei, *Z. Phys.*, 1972, **255**, 146–160.
- 32 J. H. Lee, S. M. Choi, C. Doe, A. Faraone, P. A. Pincus and S. R. Kline, *Phys. Rev. Lett.*, 2010, **105**, 038101.
- 33 M. B. Boggara, A. Faraone and R. Krishnamoorti, *J. Phys. Chem. B*, 2010, **114**, 8061–8066.
- 34 Y. Zheng, M. Nagao and D. P. Bossev, *J. Phys.: Condens. Matter*, 2009, **21**, 155104.
- 35 L. R. Arriaga, I. L. Montero, F. Monroy, G. O. Gil, B. Farago and T. Hellweg, *Biophys. J.*, 2009, **96**, 3629–3637.
- 36 B. A. Brüning, S. Prévost, R. Stehle, R. Steitz, P. Falus, B. Farago and T. Hellweg, *Biochim. Biophys. Acta*, 2014, **1838**, 2412–2419.
- 37 C. L. Armstrong, W. Häußler, T. Seydel, J. Katsaras and M. C. Rheinstädter, *Soft Matter*, 2014, **10**, 2600–2611.
- 38 J. D. Nickels, X. Cheng, B. Mostofian, C. Stanley, B. Lindner and F. A. Heberle, *et al.*, *J. Am. Chem. Soc.*, 2015, **137**, 15772–15780.
- 39 M. B. Boggara and R. Krishnamoorti, *Biophys. J.*, 2010, **98**, 586–595.
- 40 L. M. Lichtenberger, Y. Zhou, V. Jayaraman, J. R. Doyen, R. G. O’Neil, E. J. Dial, D. E. Volk, D. G. Gorenstein, M. B. Boggara and R. Krishnamoorti, *Biochim. Biophys. Acta*, 2012, **1821**, 994–1002.
- 41 A. Meyer, R. M. Dimeo, P. M. Gehring and D. A. Neumann, *Rev. Sci. Instrum.*, 2003, **74**, 2759.
- 42 T. A. Heimburg, *Biophys. J.*, 2000, **78**, 1154–1165.
- 43 E. Mamontov and K. W. Herwig, A Time-of-Flight Back-scattering Spectrometer at the Spallation Neutron Source, BASIS, *Rev. Sci. Instrum.*, 2011, **82**(8), 085109.
- 44 J. Taylor, O. Arnold, J. Bilheaux, A. Buts and S. Campbell, *et al.*, *Bull. Am. Phys. Soc.*, 2012, **57**, W26.00010.
- 45 M. Ohl, M. Monkenbusch, N. Arend, T. Kozielowski, G. Vehres and C. Tiemann, *et al.*, *Nucl. Instrum. Methods Phys. Res., Sect. A*, 2012, **696**, 85.
- 46 R. T. Azuah, L. R. Kneller, Y. Qiu, P. L. W. Tregenna-Piggott, C. M. Brown, J. R. D. Copley and R. M. Dimeo, *J. Res. Natl. Inst. Stand. Technol.*, 2009, **114**, 341.
- 47 See ESI†.
- 48 A. Zilman and R. Granek, *Phys. Rev. Lett.*, 1996, **77**, 4788.
- 49 W. Rawicz, K. C. Olbrich, T. McIntosh, D. Needham and E. Evans, *Biophys. J.*, 2000, **79**, 328–339.
- 50 M. C. Watson and F. L. H. Brown, *Biophys. J.*, 2010, **98**, L9.
- 51 M. Bloom, E. Evans and O. G. Mouritsen, *Q. Rev. Biophys.*, 1991, **24**, 293.
- 52 C. H. Cho, J. Urquidi, S. Singh and G. W. Robinson, *J. Phys. Chem. B*, 1999, **103**, 1991.
- 53 J. F. Nagle and S. Tristram-Nagle, *Biochim. Biophys. Acta*, 2000, **1469**, 159–195.